On the nonlinear temperature dependence of elastic constants and wave velocities for solid media with applications to geologic materials

Jian Yang, Li-Yun Fu, Bo-Ye Fu, Zhiwei Wang, and Wanting Hou

Citation: The Journal of the Acoustical Society of America **146**, 1556 (2019); doi: 10.1121/1.5124485
View online: https://doi.org/10.1121/1.5124485
View Table of Contents: https://asa.scitation.org/toc/jas/146/3
Published by the Acoustical Society of America

On the nonlinear temperature dependence of elastic constants and wave velocities for solid media with applications to geologic materials

Jian Yang[a] and Li-Yun Fu[b]
State Key Laboratory of Ore Deposit Geochemistry, Institute of Geochemistry, Chinese Academy of Sciences, 99 Lincheng West Road, Guanshanhu District, Guiyang 550081, China

Bo-Ye Fu[a] and Zhiwei Wang[a]
Key Laboratory of Earth and Planetary Physics, Institute of Geology and Geophysics, Chinese Academy of Sciences, 19 Beitucheng Western Road, Chaoyang District, Beijing 100029, China

Wanting Hou
Key Laboratory of Deep Oil and Gas, China University of Petroleum (East China), 66 Changjiang West Road, Huangdao District, Qingdao 266580, China

(Received 3 April 2019; revised 12 July 2019; accepted 14 August 2019; published online 5 September 2019)

Temperature-induced variations of elastic moduli in solid media are generally characterized by a strong nonlinear dependence on temperature associated with complex deformations under thermal treatments. Conventional thermoelasticity with third-order elastic constants for the one-order temperature dependence has been extensively studied for crystals, but encountering problems of divergent and limited velocity variations for rocks as a polycrystal mixture, especially at high temperatures. The extension of the theory beyond high-order elastic constants to solid media is addressed in this article to describe the nonlinear temperature dependence of both elastic constants and wave velocities. The total strain is divided into the background component associated with temperature variations and the infinitesimal component induced by propagating waves. A third-order temperature dependence of velocity variations is formulated by taking into account fourth-order elastic constants. Applications to solid rocks (sandstone, granite, and olivine) demonstrate an accurate description of temperature-induced variations, especially for high temperatures. Unlike crystals, the synthetic averaging elastic constants for a solid rock (as a polycrystal mixture) change less than 10% with temperatures. The thermal sensitivity of *P*-wave velocities is much more than that of *S*-wave velocities over the vast majority of temperatures examined.
 https://doi.org/10.1121/1.5124485

[MD] Pages: 1556–1567

I. INTRODUCTION

For most crystals, the temperature dependence of elastic constants is generally linear and weak at low temperatures, but become significant with increasing temperatures. The typical temperature behavior of elastic constants has been extensively studied for crystals, but with few publications for rocks as a polycrystal mixture. Actually, the study of temperature-induced velocity variations in a thermoelastic solid has a significant influence on several disciplines such as geothermal studies (Kristinsdóttir *et al.*, 2010), seismic exploration (e.g., Savage, 1966; Armstrong, 1984), and earthquake seismology (Boschi, 1973). At present, we still lack related advances for theoretical prediction in this field. In this article, more quantitative assessments will be conducted on the temperature dependence of elastic constants and elastic moduli in solid media, with an attempt to provide insight into the temperature-induced variations of elastic wave velocities in realistic media.

By means of ultrasonic measurements (McSkimin, 1953; McSkimin and Andreatch, 1962), the temperature dependence of elastic constants has been extensively investigated by taking into account the second-, third-, fourth-, and higher-order elastic constants for various crystals and monocrystal minerals (e.g., Hiki and Granato, 1966; Loje and Schuele, 1970; McSkimin and Andreatch, 1972; Garber and Granato, 1975a,b; Shrivastava, 1980). The relations obtained for the temperature dependence of elastic constants, however, are too complicated, especially at high temperatures. Sorokin *et al.* (1999) propose a simpler theory based on the small-amplitude bulk acoustic wave (BAW) propagating in crystals to explain the linear temperature dependence of second-order elastic constants. The first-order temperature dependence of elastic constants can be obtained by taking into account the third-order elastic constants, which, however, basically remain in the category of linear dependences. The method has been extended for a broad temperature band to quantify the nonlinear temperature dependence of elastic constants in cubic crystals (Telichko and Sorokin, 2015) by

[a]Also at: University of Chinese Academy of Sciences, 19(A) Yuquan Road, Shijingshan District, Beijing100049, China.
[b]Also at: Key Laboratory of Deep Oil and Gas, China University of Petroleum (East China), 66 Changjiang West Road, Huangdao District, Qingdao 266580, China. Electronic mail: lfu@upc.edu.cn

taking into account the fourth-order elastic constants, as well as the nonlinearity in the thermal-expansion temperature dependence. Nevertheless, these approaches concentrate on elastic constants for crystals. The extension to solid rocks, with temperature-induced velocity variations involved, is necessary to improve the theoretical prediction of experimental data in rocks.

In thermoacoustics, Biot (1956) proposes the theory of thermoelasticity on the basis of the thermodynamic of irreversible process. Deresiewicz (1957) investigates the propagation of waves in an isotropic thermoelastic solid by plane-wave analyses. Many subsequent studies have contributed to the temperature dependence of elastic constants and the thermoelastic response of an elastic medium with variable material properties (e.g., Ezzat *et al.*, 2004; Youssef, 2005; Aouadi, 2006; Othman and Kumar, 2009; Zenkour and Abbas, 2013). Some investigations (e.g., Dodson and Inman, 2013, 2014) on the thermal sensitivity of Lamb waves for aluminum give insight to how temperature affects Lamb wave speeds in different frequency ranges but with few examining temperature-associated velocity variations of elastic waves for solid rocks.

In general, the total elastic deformation for wave propagation in thermoelastic media consists of two different parts, temperature-associated and wave-associated deformations. In this study, we decompose the total strain into two components, the temperature-induced background component and the infinitesimal part induced by wave propagation. We formulate a third-order temperature dependence of velocity variations to explain the nonlinear temperature effect on elastic waves in solid rocks. The nonlinear thermoelasticity method is validated by ultrasonic experimental results with three different rocks. We demonstrate that the linear theoretical prediction of experimental data becomes significantly worse for the regime of nonlinear elastic deformations at high temperatures, whereas the nonlinear thermoelasticity method agrees with measurements more accurately, especially for larger nonlinear elastic strains by higher temperature variations. This study is also expected to improve the theoretical knowledge of preheated solid media such as sandstone, granite, and olivine rocks.

The article is organized as follows. After briefly introducing the basic principle of thermoelasticity, we formulate the strain-stress constitutive for wave propagation in thermoelastic media by strain decomposition. Next, we develop the nonlinear third-order temperature dependence of elastic wave velocities after a simple introduction of the traditional linear thermoelasticity approach. Comparisons between theoretical predictions and ultrasonic measurements with three kinds of rocks demonstrate that the proposed method gives a more accurate description of temperature-induced velocity variations than the traditional linear thermoelasticity approach, especially at high temperatures that cause larger nonlinear elastic strains. Finally, we give a discussion on elastic constants, thermal stresses, and volume thermal-expansion coefficients.

II. METHODOLOGY

A. Energy function for the strain-stress constitutive

Based on the Clausius inequality, the stress tensor σ_{ij} can be expressed as

$$\sigma_{ij} = \frac{\partial \Psi}{\partial \gamma_{ij}}, \tag{1}$$

where γ_{ij} is the strain tensor. $\Psi = \Psi(\gamma_{ij}, \theta^*)$ is the Helmholtz free energy per unit volume, and the dimensionless parameter θ^* is defined as $\theta^* = \theta/T_0$ with the temperature variation $\theta = T - T_0$ (T_0 and T are the reference and absolute temperatures, respectively). To obtain the strain-stress constitutive equation for an isotropic material, the Helmholtz free energy can be expanded in a power series with respect to θ^* and γ_{ij}, as in the following form (e.g., Dillon, 1962; Oden, 1972):

$$\begin{aligned}\Psi(\gamma_{ij}, \theta^*) = {} & a_0 + a_1 I_1 + a_2 I_2 + a_3 I_3 + a_4 \theta^* + a_5 I_1^2 \\ & + a_6 \theta^{*2} + a_7 I_1 \theta^* + a_8 I_1^3 + a_9 I_1 I_2 + \cdots,\end{aligned} \tag{2}$$

where $a_0, a_1, \ldots, a_9$ are the material constants, and I_1, I_2, I_3 are the invariants of strain tensors, which are written as follows:

$$\begin{cases} I_1 = \gamma_{ij}, \\ I_2 = \dfrac{1}{2}(\gamma_{ii}\gamma_{jj} - \gamma_{ij}\gamma_{ji}), \\ I_3 = \det \gamma_{ij}. \end{cases} \tag{3}$$

It should be noted that the effect of products of the dimensionless temperature increment θ^* over the fourth order as well as those of the strain tensor γ_{ij} over the third order could be neglected for Eq. (2) (Gatewood, 1957), the strain energy function $\Psi = \Psi(\gamma_{ij}, \theta^*)$ can be simplified in the following form:

$$\begin{aligned}\Psi(\gamma_{ij}, \theta^*) = {} & a_1 + a_2\theta^* + a_3\theta^{*2} + a_4\theta^{*3} + a_5\theta^{*4} + a_6 I_1 \\ & + a_7 I_1\theta^* + a_8 I_1\theta^{*2} + a_9 I_1\theta^{*3} + a_{10} I_1^2 \\ & + a_{11} I_1^2\theta^* + a_{12} I_1^2\theta^{*2} + a_{13} I_1^3 + a_{14} I_1^3\theta^* \\ & + a_{15} I_2 + a_{16} I_2\theta^* + a_{17} I_2\theta^{*2} + a_{18} I_1 I_2 \\ & + a_{19} I_1 I_2\theta^* + a_{20} I_3 + a_{21} I_3\theta^*.\end{aligned} \tag{4}$$

The stress-strain constitutive is given by the following relation (e.g., Wang, 1988; Kostek *et al.*, 1993):

$$\sigma_{ij} = \frac{\partial \Psi}{\partial \gamma_{ij}} = \frac{\partial \Psi}{\partial I_1}\frac{\partial I_1}{\partial \gamma_{ij}} + \frac{\partial \Psi}{\partial I_2}\frac{\partial I_2}{\partial \gamma_{ij}} + \frac{\partial \Psi}{\partial I_3}\frac{\partial I_3}{\partial \gamma_{ij}}. \tag{5}$$

Substituting Eq. (4) into Eq. (5), we have

$$\begin{aligned}\sigma_{ij} = {} & \delta_{ij}\left[a_6 + a_7\theta^* + a_8\theta^{*2} + a_9\theta^{*3}\right] \\ & + \left[2\left(a_{10} + a_{11}\theta^* + a_{12}\theta^{*2}\right)\right. \\ & \left. + \left(a_{15} + a_{16}\theta^* + a_{17}\theta^{*2}\right)\right]\gamma_{kk}\delta_{ij} \\ & - \left(a_{15} + a_{16}\theta^* + a_{17}\theta^{*2}\right)\gamma_{ij},\end{aligned} \tag{6}$$

where δ_{ij} is the Kronecker delta, and a_6 is zero in the natural state, which is regarded as the initial normal stress (Hu *et al.*, 2018).

By introducing the Lame constants μ and λ and the thermoelastic coupling coefficient β, the temperature-dependent constitutive equation is written as

$$\sigma_{ij} = \left(\lambda_2\theta^{*2} + \lambda_1\theta^* + \lambda_0\right)\gamma_{kk}\delta_{ij} + 2\left(\mu_2\theta^{*2} + \mu_1\theta^* + \mu_0\right)\gamma_{ij} - \left(\beta_2\theta^{*2} + \beta_1\theta^* + \beta_0\right)\theta\delta_{ij}, \tag{7}$$

where $\beta_0 = -(a_7/T_0)$, $\lambda_0 = a_{15} + 2a_{10}$, and $\mu_0 = -(a_{15}/2)$ are the initial values at the reference temperature T_0. The same form of material properties, $\beta_1 = -(a_8/T_0)$, $\beta_2 = -(a_9/T_0)$, $\lambda_1 = 2a_{11} + a_{16}$, $\lambda_2 = 2a_{12} + a_{17}$, $\mu_1 = -(a_{16}/2)$, and $\mu_2 = -(a_{17}/2)$, are considered as the influencing factors due to the temperature deviation.

The general formula of Eq. (7) can be rewritten as follows:

$$\sigma_{ij} = \lambda(\theta)\gamma_{kk}\delta_{ij} + 2\mu(\theta)\gamma_{ij} - \beta(\theta)\theta\delta_{ij}, \tag{8}$$

where the temperature-dependent material constants can be expressed as

$$\begin{cases} \lambda(\theta) = \lambda_2\theta^{*2} + \lambda_1\theta^* + \lambda_0 = \lambda, \\ \mu(\theta) = \mu_2\theta^{*2} + \mu_1\theta^* + \mu_0 = \mu, \\ \beta(\theta) = \beta_2\theta^{*2} + \beta_1\theta^* + \beta_0 = \beta. \end{cases} \tag{9}$$

The strain-stress constitutive is given by the following relation:

$$\gamma_{ij} = -\frac{\lambda}{2\mu(3\lambda + 2\mu)}\sigma_{kk}\delta_{ij} + \frac{1}{2\mu}\delta_{ij} + \frac{\beta}{3\lambda + 2\mu}\theta\delta_{ij}. \tag{10}$$

The coefficient of linear thermal expansion (LTE) is defined as

$$\zeta_{ij} = \frac{\partial\gamma_{ij}}{\partial\theta}. \tag{11}$$

Substituting Eq. (10) into Eq. (11), we have

$$\zeta_{ij} = \frac{\beta}{3\lambda + 2\mu}\delta_{ij} = \zeta\delta_{ij}. \tag{12}$$

The strain-stress constitutive can be rewritten as follows:

$$\gamma_{ij} = -\frac{\lambda}{2\mu(3\lambda + 2\mu)}\sigma_{kk}\delta_{ij} + \frac{1}{2\mu}\delta_{ij} + \zeta\theta\delta_{ij}. \tag{13}$$

B. Strain variations versus temperature

According to the strain-stress constitutive for isotropic material, the total strain for wave propagation in thermoelastic media can be divided into two parts,

$$\varepsilon_{ij} = \varepsilon_{ij}^1 + \varepsilon_{ij}^2. \tag{14}$$

The superscripts "1" and "2" stand for the large background strain associated with temperature variations and the infinitesimal strain induced by propagating waves, respectively. The latter is characteristic of small amplitudes in a uniform deformation (e.g., Thurston and Brugger, 1964; Sorokin *et al.*, 1999; Telichko and Sorokin, 2015; Fu and Fu, 2017).

Based on the assumption for temperature variations, ε_{ij}^1 can be written as

$$\varepsilon_{ij}^1 = \alpha\delta_{ij}, \tag{15}$$

where α indicates a positive strain induced by temperature variations. According to the research on thermoelasticity (e.g., Sorokin *et al.*, 1999; Telichko and Sorokin, 2015; Fu and Fu, 2017), the static finite-strain assumption is applied as a result of thermal expansion. Given a reasonable approximation, we have

$$\alpha = \zeta\theta, \tag{16}$$

where ζ is the coefficient of LTE, and θ is the temperature variation.

We consider a P-wave kernel, $\exp i[\omega_p t - (1+\alpha)k_p x_1]$ (Ba *et al.*, 2013), where k_p and ω_p are the wave number and angular frequency of a P-wave, respectively, i is the imaginary unit, and t is the propagating time. For a small strain ε_{ij}^2 induced by P-wave propagation, we have

$$\begin{cases} \varepsilon_{11}^2 = \gamma \exp i\left[\omega_p t - (1+\alpha)k_p x_1\right], \\ \varepsilon_{ij}^2 = 0, \ i,j \neq 1, \end{cases} \tag{17}$$

where γ is the maximum strain induced by P-wave propagation, with $\gamma \ll \alpha$.

For the expression associating ε_{ij}^2 with S-wave propagation, we consider a plane S-wave along the x_2-direction with polarization in the x_1-direction, we have

$$\begin{cases} \varepsilon_{12}^2 = \beta \exp i[\omega_s t - (1+\alpha)k_s x_2], \\ \varepsilon_{ij}^2 = 0, \ i \neq 1, \ j \neq 2, \end{cases} \tag{18}$$

where k_s and ω_s are the wave number and angular frequency of an S-wave, respectively, and β is the maximum shear strain induced by S-wave propagation, satisfying $\beta \ll \alpha$.

III. THEORETICAL PREDICTIONS AND APPLICATIONS

A. Theoretical predictions

For isotropic media, the second- and third-order elastic coefficients can be expressed by the Lame coefficients and third-order elastic constants (ν_1, ν_2, ν_3); e.g., Toupin and Bernstein, 1961; Thurston and Brugger, 1964)

$$\begin{cases} c_{11} = \lambda + 2\mu, \ \ c_{12} = \lambda, \ \ c_{44} = \mu, \\ c_{123} = \nu_1, \ \ c_{144} = \nu_2, \ \ c_{456} = \nu_3, \\ c_{112} = \nu_1 + 2\nu_2, \ \ c_{155} = \nu_2 + 2\nu_3, \ \ c_{111} = \nu_1 + 6\nu_2 + 8\nu_3. \end{cases} \tag{19}$$

According to the form of the Green–Christoffel tensor for the propagation of small-amplitude elastic waves in a crystal (Sorokin *et al.*, 1999), the linear temperature dependence of second-order elastic constants can be formulated under the action of a finite static strain. The application of the linear BAW approach to elastic wave propagation in consideration of thermal expansion tensors leads to the

following linear thermoelasticity method in terms of the third-order elastic constants:

$$\begin{cases} \rho V_p^2 = \lambda + 2\mu + \psi_1 \alpha, \\ \rho V_s^2 = \mu + \psi_2 \alpha, \end{cases} \tag{20}$$

where

$$\begin{cases} \psi_1 = 2\lambda + 4\mu + 4\nu_1 + 10\nu_2 + 8\nu_3, \\ \psi_2 = 2\mu + 3\nu_1 + 2\nu_3. \end{cases} \tag{21}$$

The BAW propagation theory has been extended to describe the nonlinear temperature dependence of elastic constants (Telichko and Sorokin, 2015) by incorporating the fourth-order elastic constants, as well as the nonlinearity of the thermal-expansion temperature dependence. Likewise, the application of the nonlinear BAW approach to elastic wave propagation results in the following nonlinear thermoelasticity method to describe the third-order temperature dependence of elastic waves velocities:

$$\begin{cases} \rho V_p^2 = \lambda + 2\mu + \gamma_1^p \alpha + \gamma_2^p \alpha^2 + \gamma_3^p \alpha^3, \\ \rho V_s^2 = \mu + \gamma_1^s \alpha + \gamma_2^s \alpha^2 + \gamma_3^s \alpha^3, \end{cases} \tag{22}$$

where $(\gamma_1^p, \gamma_2^p, \gamma_3^p)$ and $(\gamma_1^s, \gamma_2^s, \gamma_3^s)$ are the synthetic fourth-order elastic constants for *P*- and *S*- waves, respectively.

Both the third-order elastic constants $(\lambda, \mu, \nu_1, \nu_2, \nu_3)$ in Eq. (19) and the fourth-order elastic constants $(\gamma_1^p, \gamma_2^p, \gamma_3^p, \gamma_1^s, \gamma_2^s, \gamma_3^s)$ in Eq. (22) can be calculated using the best fit of ultrasonic measurements with least-squares methods. In conclusion, the linear thermoelasticity method is applicable to the deformation with elastic strains at low temperatures. With increasing temperatures and followed by thermal expansion, the resultant nonlinear elastic strains invoke to apply the nonlinear thermoelasticity method.

B. Application to sandstone samples

We use experimental data of the Dholpur sandstone (Sirdesai *et al.*, 2018) to compare the linear and nonlinear thermoelasticity methods. The result of X-ray powder diffraction (XRD) indicates that the Dholpur sandstone is monomineralic in nature, with feldspar and quartz being the primary minerals. Furthermore, the grains of feldspar and quartz are held together by siliceous cement that involves trace amounts of pyroxene and mica. The experimental temperature increases incrementally from the room temperature to 1000 °C, with a slow and constant heating rate of 5 °C/min in order to avoid undesirable extensive damage due to the formation of thermal stresses. The elastic wave velocities are determined by calculating the time required for an acoustic pulse to travel through the axial length of the sample, with two piezoelectric transducers and a waveform generator. In addition, the cylindrical sample is cut to achieve a length-to-diameter ratio of 2:1 for mechanical tests inconsistent with the ISRM (International Society for Rock Mechanics) suggested approach (Fairhurst and Hudson, 1999).

The result shows that the temperature has little effect on the bulk density of sandstone, varying from 2.22 g/cm^3 at the room temperature to 2.12 g/cm^3 at 1000 °C. The coefficient of volume thermal expansion (VTE) increases to 3.35E-05(°C^{-1}) from 25 °C to 1000 °C. The elastic constants of sandstone, obtained by a best fit of experimental measurements, including bulk density, the coefficient of VTE, and wave velocities, are listed in Table I. The *P*- and *S*- wave velocities, generally as functions of temperature (e.g., Yavuz *et al.*, 2010; Yang *et al.*, 2017), can be expressed for the Dholpur sandstone as

$$\begin{cases} V_p = 2533.66131 + 0.03305T - 0.00241T^2, \\ V_s = 1755.24766 - 0.27623T - 0.00134T^2. \end{cases} \tag{23}$$

Figure 1(a) shows the elastic wave velocities as functions of temperature for the sandstone experimental data. We see that the elastic wave velocities are kept basically constant and then increase slightly with temperatures up to 300 °C, and decrease rapidly beyond 300 °C, implying that 300 °C may be the critical temperature of damage for sandstone in the range of 300 °C–1000 °C. Figure 1(b) illustrates the thermal sensitivity of elastic wave velocities, calculated by the slope of a least-squares line fitted to velocity variations over the entire range of temperatures examined. We see that the *P*-wave velocity is more sensitive to temperature changes than the *S*-wave velocity beyond approximately 200 °C.

We use the change rate K_e to characterize the errors in velocity variations as follows:

$$K_e = \left| \frac{V_0 - V_M}{V_0} \right| \times 100\%, \tag{24}$$

where the subscript M denotes the wave velocity predicted by the linear or nonlinear thermoelasticity methods, and the subscript "0" corresponds to the experimental data.

Figures 2(a) and 2(b) compare predicted and experimental elastic wave velocities with increasing temperatures, which can be divided into three different stages. From 0 °C to 275 °C, both the theoretical predictions agree with the experimental results, with the maximum average error being 4.84%. From 275 °C to 775 °C, both the theoretical predictions basically match the experimental results with the maximum average errors of *P*- and *S*-wave velocities being 17.6% and 14.4%, respectively. The maximum average errors occur at around 675 °C and 725 °C for *P*- and *S*-waves, respectively. Beyond 775 °C, the nonlinear prediction

TABLE I. Properties of the sandstone samples.

Linear thermoelasticity theory		Nonlinear thermoelasticity theory	
λ	1.30 GPa	γ_1^p	-2.10×10^5 GPa
μ	6.50 GPa	γ_2^p	5.22×10^3 GPa
ψ_1	7.12×10^2 GPa	γ_3^p	8.06×10^2 GPa
ψ_2	3.35×10^2 GPa	γ_1^s	1.22×10^4 GPa
		γ_2^s	8.61×10^3 GPa
		γ_3^s	4.59×10^2 GPa

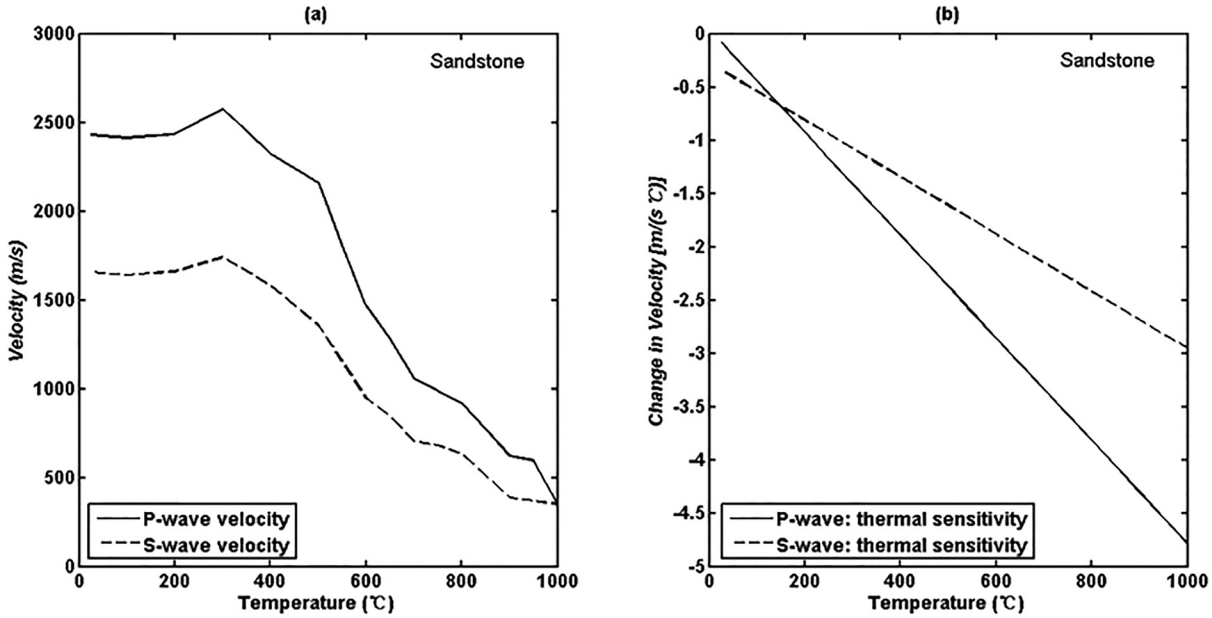

FIG. 1. Comparisons of temperature-associated velocity variations with the sandstone experimental data (a) and change in velocities with temperatures (b).

is more accurate than the linear method in describing the temperature-associated velocity variations with 32.6% maximum average error, where the linear method presents a theoretical limit against the experimental results. As a whole, the nonlinear predictions agree well with the experimental measurements, with some minor departures at different temperatures possibly because of the existence of micropores and microcracks in the sandstone before and after thermal treatments.

C. Application to granite samples

We apply two thermoelasticity methods to the temperature-associated experimental data of granite (Huang, 2014). The coupling materials used for *P*- and *S*-wave velocities are Vaseline (Unilever, London, UK) and aluminum foil, respectively. The sample with a uniform texture is normatively cut into $\phi 50 \times 100$ mm cylinders, a length-to-diameter ratio of 2:1 similar to mechanical tests, with an average bulk density of 2.73 g/cm^3 at room temperature. The main components are feldspar, amphibole, and quartz inferred from the X-ray diffraction. The thermal treatment is conducted from 20 °C to 300 °C, demonstrating a significant effect on the coefficient of VTE, from 1.73E-05($^{\circ}C^{-1}$) at 60 °C to 6.65E-05($^{\circ}C^{-1}$) at 300 °C. The elastic wave velocities are determined by ultrasonic resonance frequencies of plane-parallel thick plates. The *P*- and *S*- wave velocities can be expressed for the granite as a quadratic trend with temperature

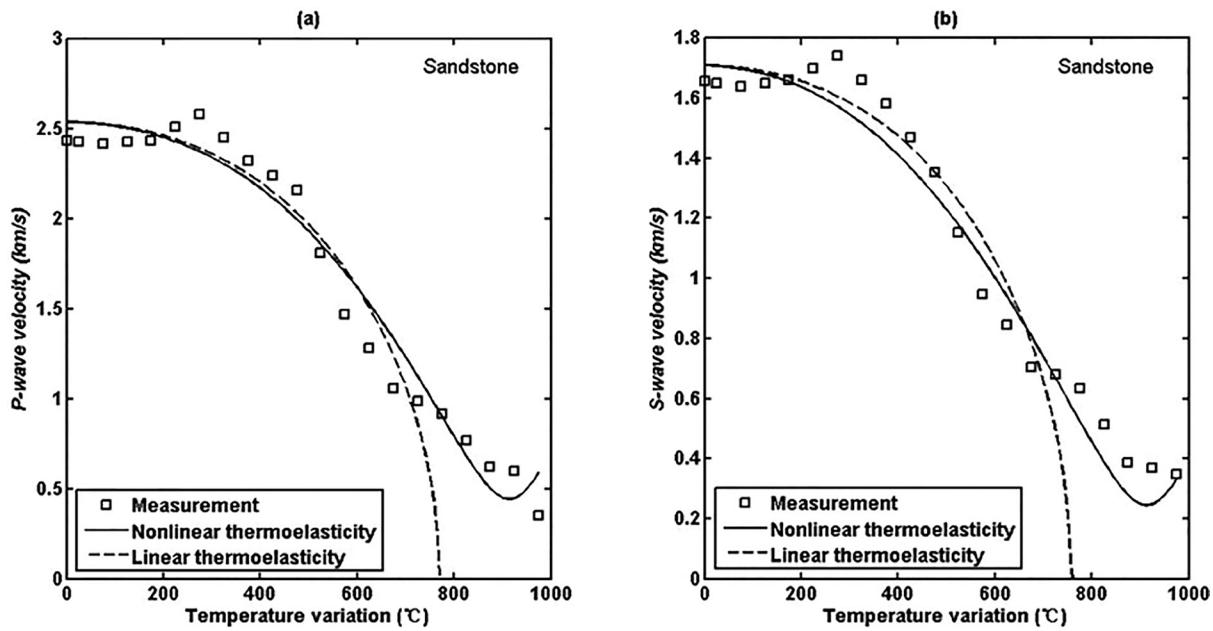

FIG. 2. Comparisons of temperature-associated velocity variations predicted by the linear and nonlinear thermoelasticity methods with the sandstone experimental data for *P*-wave velocities (a) and *S*-wave velocities (b), respectively.

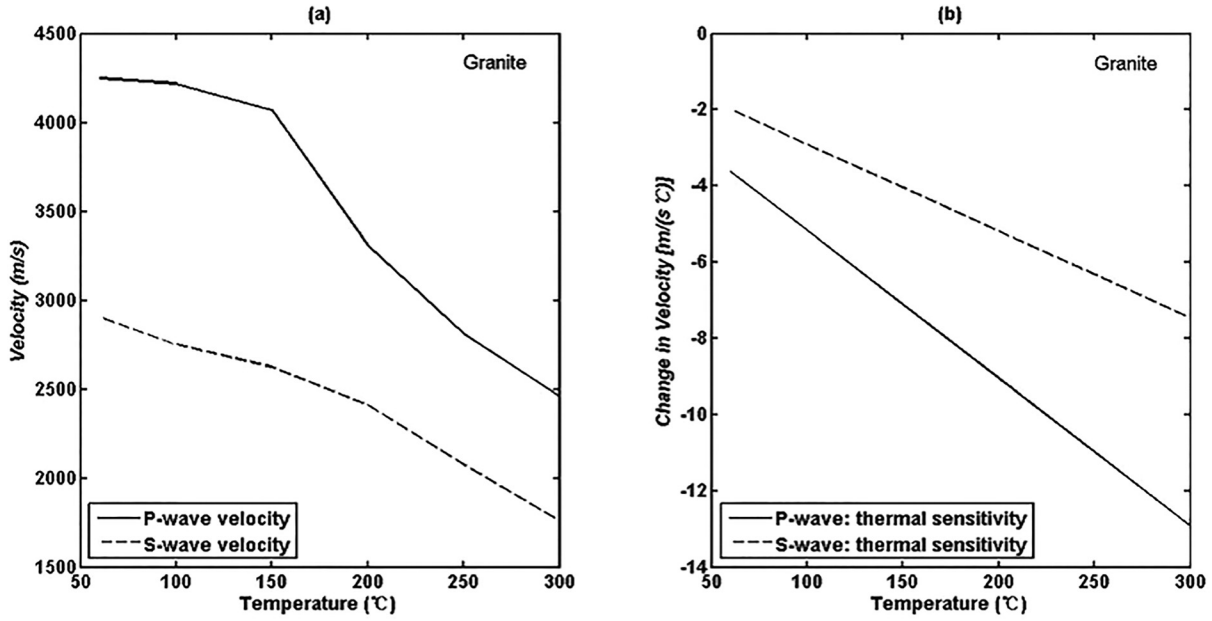

FIG. 3. Comparisons of the temperature-associated velocity variations with the granite experimental data (a) and change in velocities with temperatures (b).

$$\begin{cases} V_p = 4485.78560 - 1.29128T - 0.01940T^2, \\ V_s = 2963.36179 - 0.61085T - 0.01141T^2. \end{cases} \quad (25)$$

Figure 3(a) presents the elastic wave velocities as functions of temperature for the granite experimental data. We see that the elastic wave velocities decrease sharply with increasing temperatures. This is attributed to different minerals with different expansion coefficients and uncoordinated deformations to produce different thermal stresses in the heterogeneous granite. In general, the thermal stress affects elastic properties significantly, as well as elastic wave velocities. Figure 3(b) shows different changes of *P*- and *S*-wave velocities with temperatures. The *P*-wave velocity demonstrates greater temperature sensitivity than the *S*-wave velocity over the range of temperatures examined. The elastic constants of granite, obtained by a best fit of experimental measurements, are listed in Table II.

Figures 4(a) and 4(b) compare predicted and experimental elastic wave velocities with temperature variations, which can be divided into two different stages: 0 °C–90 °C and 90 °C–240 °C. We see that both the linear and nonlinear methods produce similar predictions for temperature-induced variations of experimental *S*-wave velocities over the range of temperatures examined, with 2.92% maximum average error probably because of the insignificant effect of low temperatures on *S*-wave velocities of granite. However, the nonlinear prediction of experimental *P*-wave velocities is much better than the linear method especially beyond 90 °C, with 3.30% and 40.3% maximum average errors, respectively.

TABLE II. Properties of the granite samples.

Linear thermoelasticity theory		Nonlinear thermoelasticity theory	
λ	5.01 GPa	γ_1^p	-1.89×10^7 GPa
μ	22.51 GPa	γ_2^p	-4.50×10^5 GPa
ψ_1	1.10×10^3 GPa	γ_3^p	-3.29×10^2 GPa
ψ_2	8.52×10^2 GPa	γ_1^s	1.66×10^6 GPa
		γ_2^s	3.43×10^4 GPa
		γ_3^s	1.02×10^3 GPa

D. Application to two olivine samples

Theoretical predictions are applied to temperature-associated experimental data of olivine rocks (Isaak, 1992). The single-crystal specimens OLA and RAM are from China and Egypt, respectively. The sample OLA consists of about 92% forsterite and 8% fayalite, whereas the sample RAM has slightly more Fe, being approximately 90% forsterite and 10% fayalite. The bulk density of specimen is measured to be from 3.330 g/cm^3 at 300 K to 3.204 g/cm^3 at 1400 K for OLA, and from 3.353g/cm^3 at 300 K to 3.213 g/cm^3 at 1500 K for RAM, respectively. The coefficient of VTE increases from 2.63E-05(K^{-1}) at 300 K to 4.00E-05(K^{-1}) at 1400 K for OLA, and from 2.63E-05(K^{-1}) at 300 K to 4.07E-05(K^{-1}) at 1500 K for RAM, respectively, implying an important influence of temperature on the VTE. The specimens are heated by an electric Rigaku DTA furnace (Rigaku, Tokyo, Japan) with a 1-MHz ultrasonic resonant frequency. Similarly, the *P*- and *S*- wave velocities of olivines can be expressed as a quadratic trend with temperature,

$$\begin{cases} V_p = 8437.15988 - 0.53117T + 1.36223T^2, \\ V_s = 4875.15844 - 0.35777T - 9.80721T^2, \end{cases} \quad (26)$$

for OLA, and

$$\begin{cases} V_p = 8357.34155 - 0.51429T - 2.28771T^2, \\ V_s = 4834.34562 - 0.35434T - 1.03896T^2, \end{cases} \quad (27)$$

for RAM.

Figures 5(a) and 6(a) denote the trend of *P*- and *S*-wave velocities over a wide range of temperatures for OLA and

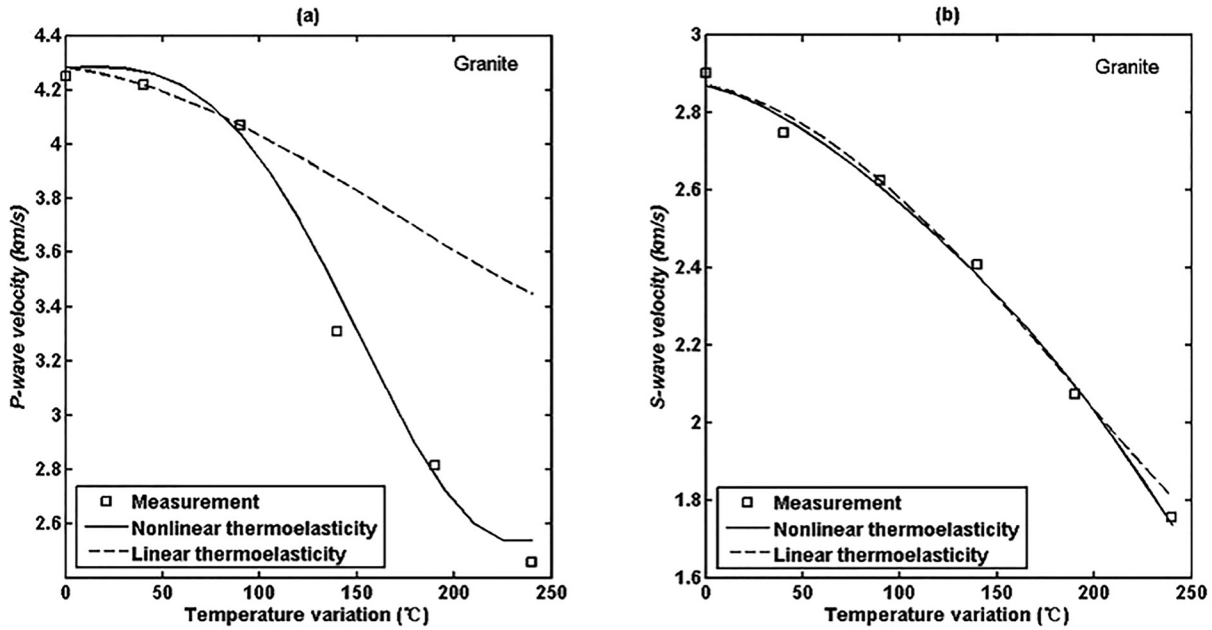

FIG. 4. Comparisons of the temperature-associated velocity variations predicted by the linear and nonlinear thermoelasticity methods with the granite experimental data for *P*-wave velocities (a) and *S*-wave velocities (b), respectively.

RAM, respectively. We see that the elastic wave velocities decrease linearly with increasing temperatures, possibly attributed to the uniform mineral composition of olivines. From the different changes of *P*- and *S*-wave velocities with temperatures, as shown in Figs. 5(b) and 6(b), we see that the *P*-wave velocity presents more temperature sensitive than the *S*-wave velocity over the entire thermal treatments. By applying Eqs. (20) and (22) to the experimental data with thermal-induced velocity variations, the best-fitting elastic constants are listed in Tables III and IV for OLA and RAM, respectively.

As shown in Figs. 7(a), 7(b), 8(a), and 8(b) for the comparison of predicted and experimental elastic wave velocities with temperature, we see that both the linear and nonlinear predictions of experimental measurements, which can also be divided into two stages, are perfect for elastic wave velocity variations from 0 °C to 500 °C/800 °C for OLA and RAM with 0.19% maximum average error, respectively. Beyond 500 °C/800 °C for OLA and RAM, respectively, however, the nonlinear thermoelasticity method becomes more accurate than the linear method, with the former less than 0.20% maximum average error and the latter up to 1.52% maximum average error. In conclusion, the nonlinear thermoelastic prediction, as expected, shows more accurate than the linear prediction, especially at high temperatures.

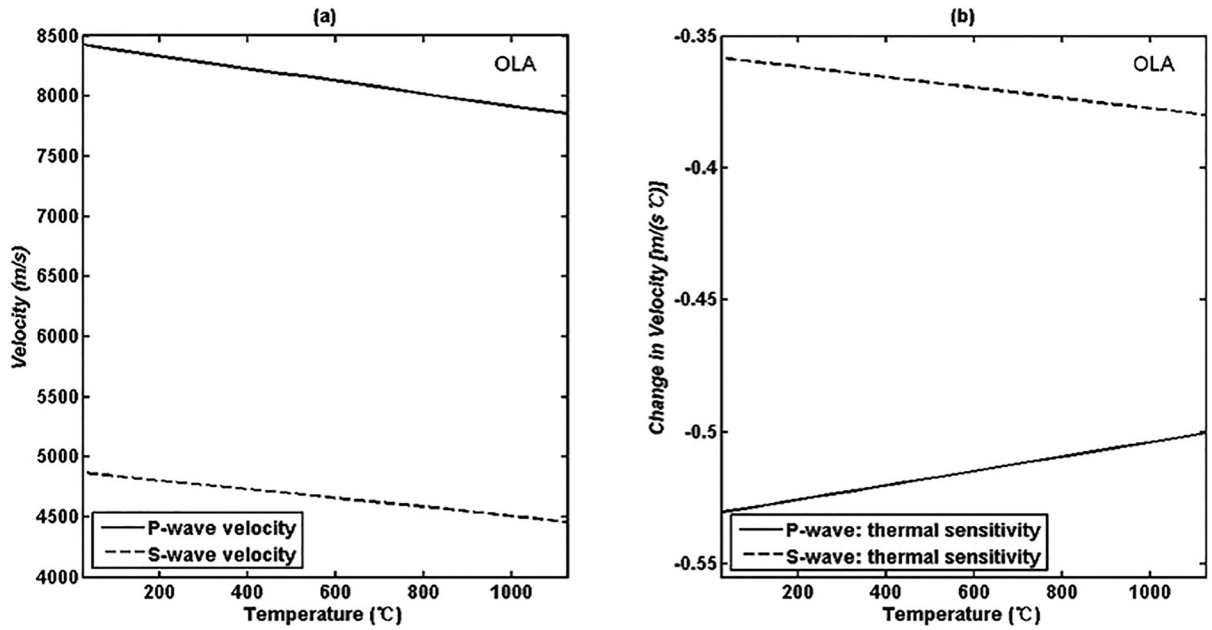

FIG. 5. Comparison of the temperature-associated velocity variations with the olivine (OLA) experimental data (a) and change in velocities with temperatures (b).

TABLE III. Properties of the olivine samples (OLA).

Linear thermoelasticity theory		Nonlinear thermoelasticity theory	
λ	77.73 GPa	γ_1^p	-5.82×10^4 GPa
μ	77.96 GPa	γ_2^p	7.81×10^3 GPa
ψ_1	-8.22×10^2 GPa	γ_3^p	-9.20×10^2 GPa
ψ_2	-3.27×10^2 GPa	γ_1^s	-3.83×10^4 GPa
		γ_2^s	3.78×10^3 GPa
		γ_3^s	-3.78×10^2 GPa

TABLE IV. Properties of the olivine samples (RAM).

Linear thermoelasticity theory		Nonlinear thermoelasticity theory	
λ	77.19 GPa	γ_1^p	-6.35×10^4 GPa
μ	77.82 GPa	γ_2^p	7.45×10^3 GPa
ψ_1	-7.74×10^2 GPa	γ_3^p	-9.32×10^2 GPa
ψ_2	-3.05×10^2 GPa	γ_1^s	-2.94×10^4 GPa
		γ_2^s	3.37×10^3 GPa
		γ_3^s	-3.75×10^2 GPa

IV. DISCUSSIONS

As is well known, the knowledge of the temperature dependence of elastic constants of solid media over a wide range of temperatures is important in characterizing temperature-associated electrical, mechanical, optical, and thermodynamic properties. In this study, we assume that the solid media (sandstone, granite, and olivine) are isotropic. We present a simple theory to describe the temperature dependence of solid-state wave velocities and elastic constants. We also consider the temperature-associated thermal stress and coefficient of VTE.

A. Temperature dependence of elastic constants with different rocks

Sorokin *et al.* (2002) demonstrate that C_{44} for three different types of quartz crystals decreases with increasing temperatures. The temperature dependence of C_{11}, C_{12}, and C_{44} for NaCl, KCl, and $\mathrm{Mo(Si,Al)_2}$, with the hexagonal C40 structure, yttrium aluminum garnet, and two grossular garnet specimen single crystals, decreases with increasing temperatures (e.g., Alton, 1967; Sharko and Botaki, 1970; Isaak *et al.*, 1992; Tanaka *et al.*, 1998). In this study, we investigate the temperature behavior of second-order elastic constants for three rocks (sandstone, granite, and olivine). It should be noted that the temperature dependence of second-order elastic constants for rocks are characteristic of a synthetic response of temperatures over different minerals as an average value. The rock sample is not a single mineral (or crystal), but a polycrystal mixture. In this case, the temperature dependence of third-order elastic constants for rocks becomes very complicated and will be addressed in the near future.

From Tables I–IV, we see that the temperature-associated elastic constants show significant changes between sandstone, granite, and olivine. As is well known, different kinds of crystals have different temperature-induced variations in elastic constants, sometimes with the deviation up to 2 orders of magnitude (e.g., Diederich and Trivisonno, 1966; Gutman and Trivisonno, 1967; Slotwinski and Trivisonno, 1969; Meeks and Arnold, 1970). However, this temperature-dependent pattern of crystals may not be valid for a rock (a polycrystal mixture). We choose some temperature points to calculate the synthetic average values of Lame constants (λ, μ) for sandstone, granite, and olivine. The results are listed in Table V, compared with Tables I–IV from the room temperature to the specified maximum temperature. We see that the temperature-associated synthetic average values of Lame constants for these polycrystal mixtures generally decrease with increasing temperatures, but with very small variations less than 10%. That is, these synthetic Lame constants listed in Tables I–IV are not largely temperature dependent. In addition, for different rocks with

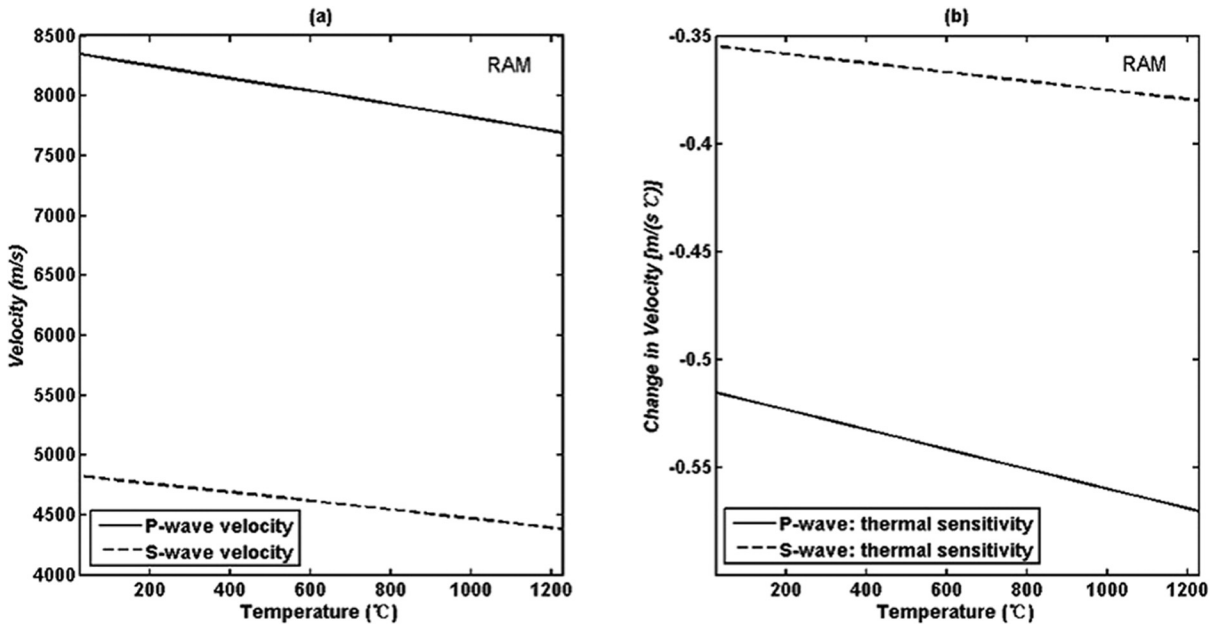

FIG. 6. Comparisons of the temperature-associated velocity variations with the olivine (RAM) experimental data (a) and change in velocities with temperatures (b).

TABLE V. Temperature dependence of elastic constants.

Elastic constants	λ	μ
Sandstone (400 °C)	1.45 GPa	6.86 GPa
Sandstone (900 °C)	1.36 GPa	6.58 GPa
OLA (600 K)	77.92 GPa	78.12 GPa
OLA (1100 K)	77.85 GPa	78.03 GPa
RAM (600 K)	77.30 GPa	78.04 GPa
RAM (1100 K)	77.22 GPa	77.87 GPa
Granite (200 °C)	5.36 GPa	23.01 GPa

different mineral formations, as different aggregations of various crystals, the temperature-associated elastic constants have big changes between each other. However, for OLA (with about 92% forsterite and 8% fayalite) and RAM (with approximately 90% forsterite and 10% fayalite), their temperature behaviors of elastic constants are quite similar, mainly caused by mineral contents with minor changes between them.

B. Thermal stress and coefficient of VTE

Thermal stress, one could say, is the stress added to a system, initially at a uniform normal temperature, if the body experiences a temperature change in the course of which it may, due to the thermal movement of its parts, be subjected to additional constraints if that stress disappears when the distribution again becomes uniform and normal (Benham *et al.*, 1964). Temperature gradients, thermal shocks, and thermal contractions can lead to thermal stress. However, there is a thermal stress important to rocks. A heterogeneous rock generally consists of different minerals with different expansion coefficients at the same temperature. Uncoordinated deformations among mineral particles lead to relative displacements between them even by small temperature changes. The resultant thermal stress induces nonlinear elastic deformations with a volumetric thermal strain, with the appearance of nonlinear elastic residual strains in thermally treated rocks (e.g., Shushakova *et al.*, 2013; Torelli *et al.*, 2017; Yang *et al.*, 2019). The thermal expansion-associated thermal stress can further cause cracks or plastic deformations depending on heating differences, material types, and constraints. The static finite strains, appearing as a result of nonlinearity of the thermal expansion temperature dependence, can be described by the coefficient of VTE.

The coefficient of VTE are defined as

$$\zeta_1 = \frac{1}{V_0}\frac{\Delta V}{\theta}, \tag{28}$$

where ΔV refers to the volume change to the initial volume at some elevated temperatures, and V_0 is the volume at an ambient reference temperature. Comparing Eq. (11) with Eq. (28), we have

$$\zeta_1 = 3\zeta + 3\zeta^2\theta^2 + 3\zeta^3\theta^3. \tag{29}$$

By ignoring high-order terms, the relationship between LTE and VTE can be simplified as follows:

$$\zeta_1 = 3\zeta. \tag{30}$$

The positive strain induced by temperature variations can be rewritten as follows:

$$\alpha = \zeta_1\theta. \tag{31}$$

As shown in Fig. 9 for the experimental data of VTE versus temperature, we see that the temperature-associated nonlinearity of VTE increases with increasing temperatures, which can be empirically fitted by a quadratic temperature function,

$$\zeta_1 = A + BT + CT^2, \tag{32}$$

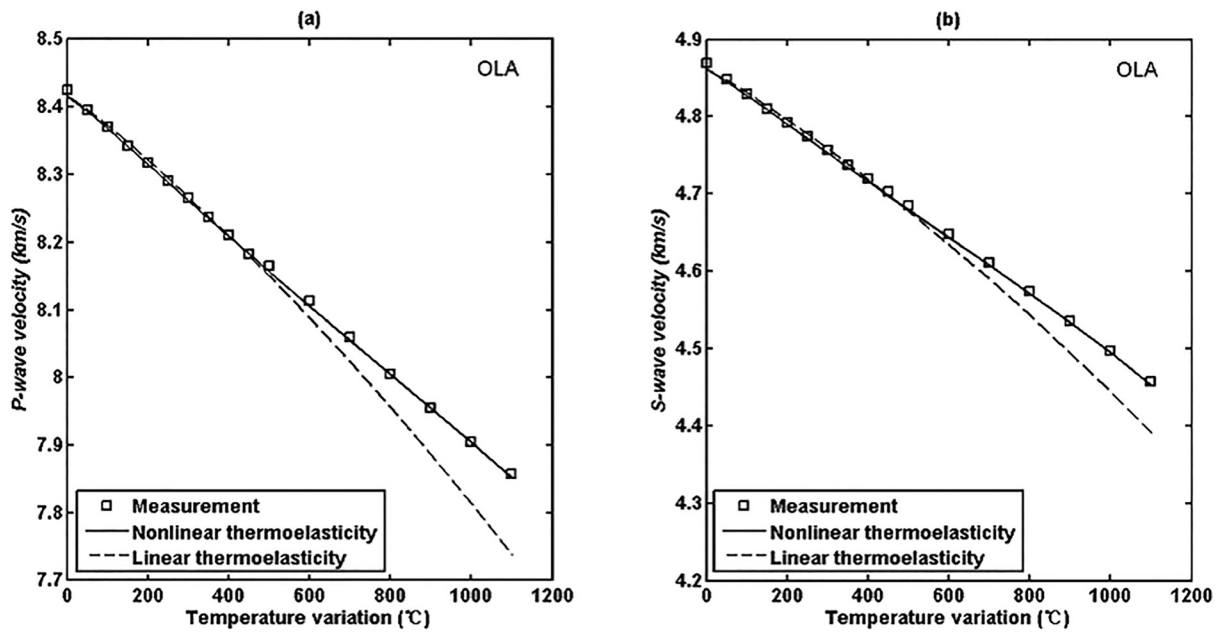

FIG. 7. Comparisons of the temperature-associated velocity variations predicted by the linear and nonlinear thermoelasticity methods with the olivine (OLA) experimental data for *P*-wave velocities (a) and *S*-wave velocities (b), respectively.

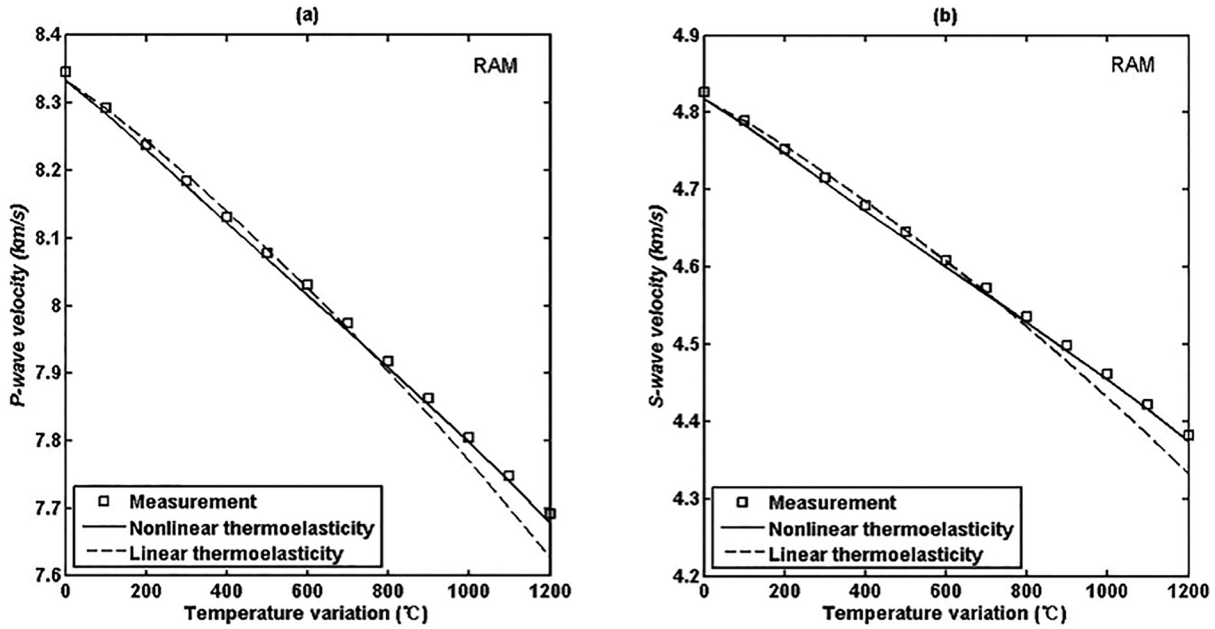

FIG. 8. Comparisons of the temperature-associated velocity variations predicted by the linear and nonlinear thermoelasticity methods with the olivine (RAM) experimental data for *P*-wave velocities (a) and *S*-wave velocities (b), respectively.

where T is the ambient reference temperature, and A, B, and C are experimental coefficients. The correlation coefficients by fitting with Eq. (32) are up to 0.949, 1.000, 0.981, and 0.979 for sandstone, granite, OLA, and RAM, respectively, indicating that the VTE could be represented by a quadratic equation (e.g., Morse and Lawson, 1967; Ma *et al.*, 2017).

Equation (32) may not be as good a representation for high temperatures, partially attributed to the difficulty in bringing the system to thermal equilibrium at high thermal temperatures. However, one would expect the thermal volume expansion coefficient to increase with temperature variations because of the exponential temperature dependence of defect formations (Morse and Lawson, 1967).

V. CONCLUSIONS

The temperature response of elastic wave velocities in rocks is extensively investigated because of the potential application to detect the temperature distribution underground. The linear thermoelasticity approach developed from the BAW propagation theory can describe the temperature-associated velocity variations of elastic waves for low temperatures. The

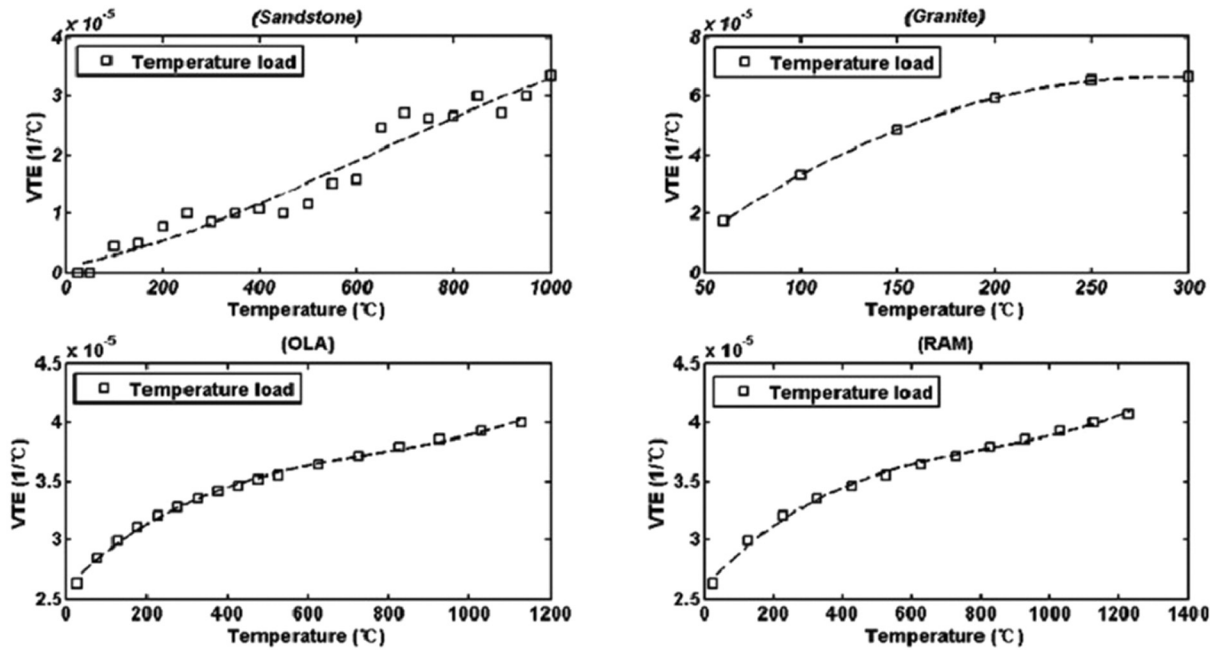

FIG. 9. Comparisons of the temperature-associated nonlinearity of VTE coefficients for sandstone (a), granite (b), OLA (c), and RAM (d).

resulting large errors to experimental data at higher temperatures have to resort to some nonlinear approaches.

We formulate a third-order temperature dependence of velocity variations by taking into account the fourth-order elastic constants. The resultant nonlinear thermoelasticity approach can describe the temperature-associated velocity variations of elastic waves at high temperatures. The main conclusions can be summarized as follows:

(1) Applications to solid rocks (sandstone, granite, and olivine) demonstrate that the nonlinear thermoelastic predictions against ultrasonic measurements are more accurate than the linear thermoelasticity approach, especially for high temperatures.
(2) For most crystals, the temperature-dependence of elastic constants is weak at low temperatures, but becomes significant at high temperatures. Unlike crystals, the synthetic averaging elastic constants for a solid rock (as a polycrystal mixture) change less than 10% with temperatures.
(3) The thermal sensitivity gives us insight into the change in *P*- and *S*-wave velocity with temperature, where the *P*-wave speed variation has a greater temperature sensitivity than the *S*-wave velocity.

ACKNOWLEDGMENTS

We thank the associate editor Michel Destrade and the two anonymous reviewers for their constructive comments. This research is supported by The National Major Project of China (Grant No. 2017ZX05008007).

Alton, W. J. (**1967**). "Temperature dependence of the elastic constants of yttrium aluminum garnet," J. Appl. Phys. **38**(7), 3023–3024.
Aouadi, M. (**2006**). "Generalized thermo-piezoelectric problems with temperature-dependent properties," Int. J. Solids Struct. **43**(21), 6347–6358.
Armstrong, B. H. (**1984**). "Models for thermoelastic attenuation of waves in heterogeneous solids," Geophys. **49**(7), 1032–1040.
Ba, J., Carcione, J. M., Cao, H., Yao, F., and Du, Q. (**2013**). "Poro-acoustoelasticity of fluid-saturated rocks," Geophys. Prospect. **61**(3), 599–612.
Benham, P. P., Hoyle, R., and Ford, H. (**1964**). *Thermal Stress* (Pitman and Sons Ltd., London).
Biot, M. A. (**1956**). "Thermoelasticity and irreversible thermodynamics," J. Appl. Phys. **27**(3), 240–253.
Boschi, E. (**1973**). "A thermoviscoelastic model of the earthquake source mechanism," J. Geophys. Res. **78**(32), 7733–7737, https://doi.org/10.1029/JB078i032p07733.
Deresiewicz, H. (**1957**). "Plane waves in a thermoelastic solid," J. Acoust. Soc. Am. **29**(2), 204–209.
Diederich, M. E., and Trivisonno, J. (**1966**). "Temperature dependence of the elastic constants of sodium," J. Phys. Chem. Solids. **27**(4), 637–642.
Dillon, O. W. (**1962**). "A nonlinear thermoelasticity theory," J. Mech. Phys. Solids. **10**(2), 123–131.
Dodson, J. C., and Inman, D. J. (**2013**). "Thermal sensitivity of Lamb waves for structural health monitoring applications," Ultrasonics. **53**(3), 677–685.
Dodson, J. C., and Inman, D. J. (**2014**). "Investigating the thermally induced acoustoelastic effect in isotropic media with Lamb waves," J. Acoust. Soc. Am. **136**(5), 2532–2543.
Ezzat, M. A., El-Karamany, A. S., and Samaan, A. A. (**2004**). "The dependence of the modulus of elasticity on reference temperature in generalized thermoelasticity with thermal relaxation," Appl. Math Comput. **147**(1), 169–189.
Fairhurst, C. E., and Hudson, J. A. (**1999**). "Draft ISRM suggested method for the complete stress-strain curve for the intact rock in uniaxial compression," Int. J. Rock Mech. Min. Sci. **36**(3), 279–289.
Fu, B. Y., and Fu, L. Y. (**2017**). "Poro-acoustoelastic constants based on Padé approximation," J. Acoust. Soc. Am. **142**(5), 2890–2904.
Garber, J. A., and Granato, A. V. (**1975a**). "Theory of the temperature dependence of second order elastic constants in cubic materials," Phys. Rev. B. **11**(10), 3990–3997.
Garber, J. A., and Granato, A. V. (**1975b**). "Fourth-order elastic constants and the temperature dependence of second-order elastic constants in cubic materials," Phys. Rev. B. **11**(10), 3998–4007.
Gatewood, B. E. (**1957**). *Thermal Stress* (McGraw-Hill, New York).
Gutman, E. J., and Trivisonno, J. (**1967**). "Temperature dependence of elastic constants of rubidium," J. Phys. Chem. Solids. **28**, 805–809.
Hiki, Y., and Granato, A. V. (**1966**). "Anharmonicity in noble metals; higher order elastic constants," Phys. Rev. **144**(2), 411–419.
Hu, Y. J., Liu, F., Zhu, W. D., and Zhu, J. M. (**2018**). "Thermally coupled constitutive relations of thermoelastic materials and determination of their material constants based on digital image correlation with a laser engraved speckle pattern," Mech. Mater. **121**, 10–20.
Huang, H. (**2014**). "The damage research of granite with thermal elastic brittle quality and the analysis of borehole wall stability," Master's thesis, China University of Geosciences, Beijing.
Isaak, D. G. (**1992**). "High-temperature elasticity of iron-bearing olivines," J. Geophys. Res. Sol. Ea. **97**(B2), 1871–1885, https://doi.org/10.1029/91JB02675.
Isaak, D. G., Anderson, O. L., and Oda, H. (**1992**). "High-temperature thermal expansion and elasticity of calcium-rich garnets," Phys. Chem. Minerals. **19**, 106–120.
Kostek, S., Sinha, B. K., and Norris, A. N. (**1993**). "Third-order elastic constants for an inviscid fluid," J. Acoust. Soc. Am. **94**(5), 3014–3017.
Kristinsdóttir, L. H., Flóvenz, Ó. G., Árnason, K., Bruhn, D., Milsch, H., Loje, K. F., and Schuele, D. E. (**2010**). "Electrical conductivity and P-wave velocity in rock samples from high-temperature Icelandic geothermal fields," Geothermics **39**(1), 94–105.
Loje, K. F., and Schuele, D. E. (**1970**). "The pressure and temperature derivatives of the elastic constants of AgBr and AgCl," J. Phys. Chem. Solids. **31**(9), 2051–2067.
Ma, Z. G., Tang, F. R., Qi, F. Z., Shi, X. D., Xiang, H., and Lian, Y. Q. (**2017**). "Experimental study on thermal expansion coefficient changing rule of sandstone under high temperature," J. Min. Safety Eng. **34**(1), 121–126.
McSkimin, H. J. (**1953**). "Measurement of elastic constants at low temperatures by means of ultrasonic waves—Data for silicon and germanium single crystals, and for fused silica," J. Appl. Phys. **24**(8), 988–997.
McSkimin, H. J., and Andreatch, P. (**1962**). "Analysis of the pulse superposition method for measuring ultrasonic wave velocities as a function of temperature and pressure," J. Acoust. Soc. Am. **34**(5), 609–615.
McSkimin, H. J., and Andreatch, P. (**1972**). "Elastic moduli of diamond as a function of pressure and temperature," J. Appl. Phys. **43**(7), 2944–2948.
Meeks, E. L., and Arnold, R. T. (**1970**). "Temperature dependence of the third-order elastic constants of SrTi," Phys. Rev. B. **1**(3), 982–988.
Morse, G. E., and Lawson, A. W. (**1967**). "The temperature and pressure dependence of the elastic constants of thallium bromide," Solid State Commun. **5**(2), 939–950.
Oden, J. T. (**1972**). *The Finite Elements of Nonlinear Continua* (McGraw-Hill, New York).
Othman, M. I. A., and Kumar, R. (**2009**). "Reflection of magneto-thermoelasticity waves with temperature dependent properties in generalized thermoelasticity," Int. Commun. Heat Mass. **36**(5), 513–520.
Savage, J. C. (**1966**). "Thermoelastic attenuation of elastic waves by cracks," J. Geophys. Res. **71**(16), 3929–3938, https://doi.org/10.1029/JZ071i016p03929.
Sharko, A. V., and Botaki, A. A. (**1970**). "Temperature dependence of the elastic constants and Debye temperature of NaCl and KCl single crystals," Russ. Phys. J. **13**(6), 708–712.
Shrivastava, U. C. (**1980**). "Temperature dependence of the elastic constants of alkali halides," Phys. Rev. B. **21**(6), 2602–2606.
Shushakova, V., Fuller, E. R., Heidelbach, F., Mainprice, D., and Siegesmund, S. (**2013**). "Marble decay induced by thermal strains: Simulations and experiments," Environ. Earth Sci. **69**(4), 1281–1297.
Sirdesai, N. N., Singh, A., Sharma, L. K., Singh, R., and Singh, T. N. (**2018**). "Determination of thermal damage in rock specimen using intelligent techniques," Eng. Geol. **239**, 179–194.

Slotwinski, T., and Trivisonno, J. (**1969**). "Temperature dependence of the elastic constants of single crystal lithium," J. Phys. Chem. Solids. **30**(5), 1276–1278.
Sorokin, B. P., Glushkov, D. A., and Aleksandrov, K. S. (**1999**). "Temperature dependence of the second-order elastic constants of cubic crystals," Phys. Solid State. **41**(2), 208–212.
Sorokin, B. P., Glushkov, D. A., Turchin, P. P., Michailyuta, S. V., Aleksandrov, K. S., and Doubovsky, A. B. (**2002**). "Elastic anharmonicity and elastic constants temperature dependences of different quality quartz crystals," in *IEEE/EIA International Frequency Control Symposium and Exhibition*, pp. 410–415.
Tanaka, K., Nawata, K., Inui, H., Yamagchi, M., and Koiwa, M. (**1998**). "Temperature dependence of single-crystal elastic constants of Mo(Si, Al)$_2$," Intermetallics. **6**(7-8), 607–611.
Telichko, A. V., and Sorokin, B. P. (**2015**). "Extended temperature dependence of elastic constants in cubic crystals," Ultrasonics **61**, 1–5.
Thurston, R. N., and Brugger, K. (**1964**). "Third-order elastic constants and the velocity of small amplitude elastic waves in homogeneously stressed media," Phys. Rev. **135**(6A), A1604–A1610.
Torelli, G., Gillie, M., Mandal, P., and Tran, V. X. (**2017**). "A multiaxial load-induced thermal strain constitutive model for concrete," Int. J. Solids Struct. **108**, 115–125.
Toupin, R. A., and Bernstein, B. (**1961**). "Sound waves in deformed perfectly elastic materials: Acoustoelastic effect," J. Acoust. Soc. Am. **33**(2), 216–225.
Wang, H. G. (**1988**). "The expression of free energy for thermoelastic material and its relation to the variable material coefficients," Appl. Math. Mech. **9**(12), 1073–1078.
Yang, J., Fu, L. Y., Zhang, W. Q., and Wang, Z. W. (**2019**). "Mechanical property and thermal damage factor of limestone at high temperature," Int. J. Rock Mech. Min. **117**, 11–19.
Yang, S. Q., Xu, P., Li, Y. B., and Huang, Y. H. (**2017**). "Experimental investigation on triaxial mechanical and permeability behavior of sandstone after exposure to different high temperature treatments," Geothermics. **69**, 93–109.
Yavuz, H., Demirdag, S., and Caran, S. (**2010**). "Thermal effect on the physical properties of carbonate rocks," Int. J. Rock Mech. Min. **47**(1), 94–103.
Youssef, H. M. (**2005**). "Dependence of modulus of elasticity and thermal conductivity on reference temperature in generalized thermoelasticity for an infinite material with a spherical cavity," Appl. Math. Mech. **26**, 470–475.
Zenkour, A. M., and Abbas, I. A. (**2013**). "A generalized thermoelasticity problem of an annular cylinder with temperature-dependent density and material properties," Int. J. Mech. Sci. **84**, 54–60.